

QUANTUM SUPPRESSION OF BEAMSTRAHLUNG FOR FUTURE e^+e^- LINEAR COLLIDERS

MING XIE

*Lawrence Berkeley National Laboratory
Berkeley, CA 94720, USA
E-mail: mingxie@lbl.gov*

Beamstrahlung at interaction point may present severe limitations on linear collider performance. The approach to reduce this effect adopted for all current designs at a center-of-mass energy of 0.5 TeV will become more difficult and less effective at higher energy. We discuss the feasibility of an alternative approach, based on an effect known as quantum suppression of beamstrahlung, for future linear colliders at multi-TeV energy.

1 Introduction

One of the most important constraint on the performance of a e^+e^- linear collider is that imposed by the QED processes¹, in particular beamstrahlung^{2,3,4,5,6,7,8}, at the Interaction Point (IP). Beamstrahlung is the synchrotron radiation produced by the particles of one beam as they pass through the electric and magnetic fields of the oncoming beam. The fields can be so strong due to the extremely high charge density that colliding particles may lose significant amount of their energy, causing severe luminosity degradation. The photons generated by beamstrahlung may also turn to copious e^+e^- pairs, or even hadrons in the form of minijets through QCD processes, causing troublesome background problem to the detectors and the particle physics under study. Therefore a crucial task to assess the potential of future linear collider is to identify the operation regimes and the approaches with which the impact of these deleterious effects on collider performance can be minimized, taking into account other collider constraints and requirements, of course.

To suppress beamstrahlung, the so called flat-beam approach has been adopted for all current designs of linear collider at a center-of-mass energy of 0.5 TeV⁹. However this approach will become more difficult technically and less effective at higher energy, as will be explained later. Recently, high energy physics community has been emphasizing the importance of higher energy reach (up to 5 TeV) for a linear collider¹⁰. There is also a need to explore drastically different collider parameter regime that might potentially be reached with the advanced acceleration techniques currently under active investigation¹¹. It is now becoming increasingly important to search for more feasible IP approaches at higher energy.

Several methods have been proposed for beamstrahlung suppression in addition to the flat-beam approach. Charge compensation method^{12,13} requires the mixing of beams of opposite charge to neutralize the beam field before collision. However, due to a beam instability, imperfection in mixing could cause luminosity degradation. The beam fields may also be reduced by the return current in a plasma¹⁴ introduced at the IP. The problem of concern in this case is the hadronic background due to the collisions of beams with dense plasma ions. Instead of colliding charged particle beams, one may also convert them into photon beams to make a $\gamma\gamma$ collider¹⁵. But it seems unlikely that a $\gamma\gamma$ collider could scale more favorably to higher energy than its e^+e^- counterpart due to other technical constraints. Apart from that, $\gamma\gamma$ collision is not meant to be a substitute for e^+e^- annihilation in terms of physics discovery potential¹⁶. Regardless of the variety, the working philosophy behind all these methods is the same that is to reduce or eliminate if possible the strong beam fields. Nevertheless, there is an exception.

In this paper, we discuss an effect known as Quantum Suppression of Beamstrahlung (QSB). Unlike all other approaches, QSB is effective only when the beam field is sufficiently strong. In that regard, it is compatible with the ever increasing beam density required of a linear collider at higher energy, thus deserves a careful investigation.

A brief description of beamstrahlung and the rationale behind the interest in QSB are given in Section 2. More specific definition of QSB is explained in Section 3 after a discussion of collider scaling laws. Monte-Carlo IP simulation for a 5 TeV collider case is presented in section 4 to illustrate the characteristics of QSB and in particular the induced QED backgrounds. This then leads to a discussion of major issues involved and the uncertainties in establishing QSB as a feasible IP approach. Finally we conclude in Section 6.

2 Beamstrahlung

Beamstrahlung can be classified into three regimes¹ according to the magnitude of the beamstrahlung parameter, $\Upsilon = \gamma B/B_c$, where $\gamma = E_b/mc^2$, E_b is the beam energy, B the beam field and B_c the Schwinger critical field. The three regimes are, respectively, the classical regime if $\Upsilon \ll 1$, the extreme or strong quantum regime if $\Upsilon \gg 1$, and in between the transition regime.

In the classical regime, beamstrahlung can be calculated with the usual synchrotron radiation formula derived from classical electrodynamics. Alternatively, the beamstrahlung parameter may be expressed as $\Upsilon = 2\epsilon_c/3E$ in terms of a classical quantity known as critical photon energy, ϵ_c . The classical theory is valid only if the energy of the radiated photon, characterized by ϵ_c ,

is much less than the kinetic energy of the radiating particle. This condition corresponds to $\Upsilon \ll 1$.

So far all the designs of linear colliders at 0.5 TeV have managed to stay in the regime with $\Upsilon < 1$ ⁹, where beamstrahlung and its deleterious effects can be reduced by having smaller Υ . Therefore reducing Υ by reducing the beam field, has been adopted as a guideline and that is made possible by taking the flat beam approach. However, as we know the required luminosity for a collider has to rise as the square of its energy, thus to keep wall plug power under control the beam has to be focused to smaller size with higher charge density, this will unavoidably raise Υ and put a linear collider into the strong quantum regime. As a result the flat beam approach will become more difficult and less effective at higher energy. More difficult for technical reason, as it requires the beam size in one transverse direction to be much smaller (for given beam area), thus pushing the limit for tight beam positioning control at higher energy. For current designs at 0.5 TeV, the vertical beam size is already down to a few nanometers. Less effective for physical reason, as it has been shown³ the dependence of the spread in luminosity spectrum on beam shape becomes very weak in the strong quantum regime.

Question then arises: what would be the approach to suppress beamstrahlung at higher energy if a linear collider will be unavoidably pushed into the strong quantum regime? Fortunately, the very nature itself offers help. As Υ increases due to either stronger fields or higher energy of the beam, the radiated photons become more energetic. Quantum theory has to be used to take into account radiation recoil and the fact that photon spectrum beyond the particle energy is kinetically forbidden. A full quantum treatment of synchrotron radiation was given by Sokolov et al.¹⁷ for arbitrary value of Υ in a constant field. This result was later applied to and extended for the study of beamstrahlung^{2,3,4,5,6,7,8}.

According to the quantum theory, beamstrahlung scales differently in the regimes $\Upsilon \ll 1$ and $\Upsilon \gg 1$. It was shown² that advantage may be taken of this behavior in the extreme quantum regime to extend collider energy to multi-TeV without excessive beamstrahlung. It was also made clear that the beam parameters required to take advantage of this effect, such as very short bunch or small emittance, are not readily achievable, and the flat beam approach is a much better choice at 0.5 TeV energy range.

However, one should not forget that 0.5 TeV energy is only a near term goal for linear collider development, very much limited by the current technologies. Considering competitions from hadron or even muon colliders, it would be much more compelling for linear collider to go beyond that energy. During a recent Snowmass Workshop¹⁰ on New Directions for High-Energy Physics in

1996 and later on in the 7th Workshop on Advanced Accelerator Concepts¹¹, accelerator community has made an interesting attempt to consider various accelerator issues and IP approaches at an energy of 5 TeV.

In particular, the possibility of employing quantum suppression as an IP approach was explored over a wide range of beam parameters at 5 TeV by Xie et al.¹⁸. It was shown in this study that when the major accelerator and IP constraints are taken into account, it becomes increasingly necessary to operate linear colliders in high Υ regime and use to our advantage the quantum effect to suppress beamstrahlung. Full blown Monte-Carlo simulation was performed to study luminosity spectrum under the influence of all major EM and QED processes at the IP, including disruption, beamstrahlung, incoherent and coherent pair creations. The results was surprisingly encouraging. Later in section 4, we will summarize this work and provide additional simulations to evaluate QED backgrounds.

3 Collider Scaling

What is quantum suppression and how could it be realized in a linear collider? This question is better answered after a discussion of major accelerator and IP requirements and constraints. In this section we will start with simple formulas of collider scaling¹ and reorganize collider parameters in a way more convenient for exploration. A definition of QSB subjected to the collider constraints will be given at the end.

The primary drive for developing ever more advanced accelerators is to expand both energy and luminosity frontiers for high energy physics applications. An important collider performance parameter is the geometrical luminosity given by

$$\mathcal{L}_g = \frac{f_c N^2}{4\pi\sigma_x\sigma_y} \quad (1)$$

where f_c is the collision frequency, N the number of particles per bunch, σ_x and σ_y are, respectively, the horizontal and vertical rms beam sizes at the IP. The real luminosity, however, depends on various dynamic processes occurred during beam collision, in particular beamstrahlung and disruption. These two processes are determined by the beamstrahlung parameter

$$\Upsilon = \frac{5r_e^2\gamma N}{6\alpha\sigma_z(\sigma_x + \sigma_y)} \quad (2)$$

now averaged over a Gaussian bunch distribution, and the disruption parameter

$$D_y = \frac{2r_e N\sigma_z}{\gamma\sigma_y(\sigma_x + \sigma_y)} \quad (3)$$

where r_e is the classical electron radius, α the fine structure constant, and σ_z the rms bunch length. Disruption refers to the bending of particle trajectories due to the field of oncoming beam.

One may chose to monitor the severity of beamstrahlung by average number of emitted photons per beam particle

$$n_\gamma = 2.54 \left(\frac{\alpha \sigma_z \Upsilon}{\lambda_c \gamma} \right) U_0(\Upsilon) \quad (4)$$

and by average relative beam energy loss

$$\delta_E = 1.24 \left(\frac{\alpha \sigma_z \Upsilon}{\lambda_c \gamma} \right) \Upsilon U_1(\Upsilon) \quad (5)$$

where

$$U_0(\Upsilon) \approx \frac{1}{(1 + \Upsilon^{2/3})^{1/2}} \quad (6)$$

$$U_1(\Upsilon) \approx \frac{1}{(1 + (1.5\Upsilon)^{2/3})^2} \quad (7)$$

and $\lambda_c = \hbar/mc$ is the Compton wavelength.

To avoid significant degradation of luminosity and excessive detector backgrounds, n_γ and δ_E should be kept sufficiently small. Generally speaking, when these requirements are satisfied, other deleterious effects such as pair creation and hadronic backgrounds will also tend to be small. Another major constraint for collider design is the available beam power, limited by wall plug power given accelerator efficiency. We define the total average power of both colliding beams by $P_b = 2E_b N f_c$, and the full center-of-mass energy by $E_{cm} = 2E_b$.

It is noted from all the formulas given above that there are only six independent parameters and they are chosen for convenience to be $\{E_{cm}, \mathcal{L}_g, P_b, R, N, \sigma_z\}$, where R is the aspect ratio σ_x/σ_y . For major collider design considerations we chose to monitor these quantities $\{f_c, \sigma_y, \Upsilon, D_y, n_\gamma, \delta_E\}$, and they are expressed in terms of the six independent parameters as follows

$$f_c = \left(\frac{P_b}{E_{cm}} \right) \left(\frac{1}{N} \right) \quad (8)$$

$$\sigma_y = \left(\frac{1}{\sqrt{4\pi}} \right) \left(\frac{1}{\sqrt{R}} \right) \left(\sqrt{\frac{P_b}{E_{cm} \mathcal{L}_g}} \right) (\sqrt{N}) \quad (9)$$

$$\Upsilon = \left(\frac{5\sqrt{\pi} r_e^2}{6\alpha m c^2} \right) \left(\frac{\sqrt{R}}{1+R} \right) \left(\sqrt{\frac{E_{cm}^3 \mathcal{L}_g}{P_b}} \right) \left(\frac{\sqrt{N}}{\sigma_z} \right) \quad (10)$$

$$D_y = (16\pi m c^2 r_e) \left(\frac{R}{1+R} \right) \left(\frac{\mathcal{L}_g}{P_b} \right) (\sigma_z) \quad (11)$$

$$n_\gamma = 2.54 U_0(\Upsilon) F \quad (12)$$

$$\delta_E = 1.24 \Upsilon U_1(\Upsilon) F \quad (13)$$

$$F = \left(\frac{5\sqrt{\pi} r_e^2}{3\lambda_c} \right) \left(\frac{\sqrt{R}}{1+R} \right) \left(\sqrt{\frac{E_{cm} \mathcal{L}_g}{P_b}} \right) (\sqrt{N}). \quad (14)$$

The advantage of organizing the independent parameters and dependent quantities in such a way lies in its convenience for design optimization in multi-dimensional parameter space, since in most situations most independent parameters can be fixed. For the example given in this paper, we set $E_{cm} = 5$ TeV and $\mathcal{L}_g = 10^{35} \text{cm}^{-2} \text{s}^{-1}$ as our goals in energy and luminosity frontiers. When exploring the potential of laser-driven acceleration, it is reasonable to assume $R = 1$. Then for a reasonably small beam power at $P_b = 20$ MW we are left with only two independent parameters $\{N, \sigma_z\}$ to vary.

To see how QSB works under the collider constraints it is instructive to look at the more transparent scaling laws in two dimensional parameter space $\{N, \sigma_z\}$ when $\{E_{cm}, \mathcal{L}_g, P_b, R\}$ are considered fixed

$$f_c \sim \frac{1}{N}, \quad \sigma_y \sim \sqrt{N}, \quad D_y \sim \sigma_z, \quad \Upsilon \sim \frac{\sqrt{N}}{\sigma_z} \quad (15)$$

$$n_\gamma \sim U_0(\Upsilon) \sqrt{N}, \quad \delta_E \sim \Upsilon U_1(\Upsilon) \sqrt{N}. \quad (16)$$

In the limit $\Upsilon \gg 1$, Eqs.(6,7) give

$$U_0(\Upsilon) \rightarrow \frac{1}{\Upsilon^{1/3}}, \quad \Upsilon U_1(\Upsilon) \rightarrow \frac{1}{\Upsilon^{1/3}} \quad (17)$$

Eq.(16) becomes

$$n_\gamma \sim (N\sigma_z)^{1/3}, \quad \delta_E \sim (N\sigma_z)^{1/3}. \quad (18)$$

Notice from Eqs.(15,18) that once in the high Υ regime there are two approaches to reduce beamstrahlung: either by reducing N or by reducing σ_z . The consequences on collider design and hence the implied restrictions on the approaches, however, can be quite different. Reducing N leads to weaker beam field and a smaller Υ , while reducing σ_z leads to stronger beam field and a larger Υ . The first approach requires σ_y to be decreased and f_c increased thus the approach is limited by the constraints on σ_y and f_c , while the second approach is not directly restricted in that regard.

Here we are led to the following definition of QSB. Consider a case when all other five independent parameters of our choice are fixed except the bunch length σ_z . As a result all other beam parameters are also fixed. As σ_z decreases, the beam density hence the beam field and Υ increase, the radiative energy loss per unit time will also increase either in the extreme quantum regime or classical regime. However when multiplied by the bunch length, the radiative energy loss per bunch crossing decreases in the extreme quantum regime while still increases in the classical regime. This effect thus may be called the quantum suppression of beamstrahlung.

The QSB so defined calls for short bunch length. This is again compatible with the trend of reducing the wavelength of acceleration field from the current microwave accelerators to the future laser-driven accelerators.

4 IP Simulation in Strong Quantum Regime

In this section we present full-blown IP simulation using CAIN developed by Yokoya and co-workers¹⁹. CAIN is capable of handling all major electromagnetic and QED processes occurred at the IP, including disruption, beamstrahlung, coherent and incoherent pair creation. It is a Monte-Carlo code which follows beam particles, photons and pairs in six-dimensional phase space, as well as their spins and polarization. In comparison, the previous studies of beamstrahlung in the strong quantum regime^{2,3,4,5,6,7,8} were concentrated mainly on obtaining analytical and semi-analytical results to understand the physics, thus were limited to treating only simple, idealistic models. In these early studies, either disruption or multiple beamstrahlung or both were neglected, and none was able to treat simultaneously the pair production and give angular-momentum distributions. However this information is essential to background analysis and the overall assessment of collider performance, especially in high Υ regime. The beam parameters used for simulation in this paper are given in Table 1, which are taken from the CASE II by Xie et al¹⁸.

Figure 1 shows the luminosity spectrum for e^+e^- and $\gamma\gamma$ collisions. For e^+e^- case the spectrum is characterized by an outstanding core at the full energy and a very broad tail two orders of magnitude below the peak. Although cross sections for background events are generally higher at lower energy, this effect is significantly suppressed. The products from most collisions in the low energy tail are highly boosted due to the asymmetry in energy of the collision partners, thus are confined mostly within a small forward and backward angular cones. Seen from Table 3, the core itself within 1% of full energy accounts for 65% of the geometrical luminosity, even though on average the beam loses 26% of its energy and has a rms energy spread of 36%. The sharpness and

high peak value of the core is surprisingly encouraging. Upon careful examination, it is found that nearly half of the primary particles went through beam crossing without having enough probability to suffer energy loss through any QED process, even though their trajectories are bent significantly by the beam field. Because of quantum suppression, the number of beamstrahlung photons defined in terms of n_γ is even lower compared with most of the designs at 0.5 TeV⁹. However, the full effect of beamstrahlung has to be evaluated by examining also other characteristics of collision output.

The angle spectrum and angle-energy distribution of the photons are given in Figure 2. In the lower plot we see features of two distinct distributions. The photons generated by primary particles at full energy occupy the band below 0.2 mrad, roughly. This number corresponds to the characteristic disruption angle of primary particles given by $\theta_d = D_y\sigma_y/\sigma_z$. The photons with angle larger than 0.2 mrad are generated either through secondary beamstrahlung or by pair particles to be discussed later. The angle-energy correlation, shown more remarkably above the lower band, is due to the fact that the lower the energy of the radiating particle, the larger the angle it is deflected by the beam field, and the larger the angle of the radiated photon.

Another major source of backgrounds at high Υ is the copious coherent e^+e^- pairs created by beamstrahlung photons traveling in the strong field of the opposing beam²⁰. The number of pairs per primary particle may be estimated with a formula given by Yokoya and Chen¹

$$n_b = \left(\frac{\alpha\sigma_z\Upsilon}{\lambda_c\gamma} \right)^2 \Xi(\Upsilon) \quad (19)$$

$$\Xi(\Upsilon) = 0.295\Upsilon^{-2/3}(\log\Upsilon - 2.488) \quad (\Upsilon \gg 1). \quad (20)$$

A comparison between simple formula and simulation is given in Table 2 and Table 3 for several characteristic quantities.

In high Υ regime, coherent pair partners are more likely to share the photon energy asymmetrically²⁰, giving rise to particles with significantly lower energy. These low energy pair particles, if deflected to large enough angle, may enter the detector and cause background or even damage problems. The pair partner with the same sign as the co-moving beam sees a focusing field, while the opposite sign pair partner sees a defocusing field of the opposing beam. As a result, the angle characteristics can be quite different for different pair partners. The angle-energy distributions of coherent pairs together with beam particles are shown in Figure 3 (top). The beam particles are concentrated mostly in the area near full energy. Notice the split of two bands in the lower energy region. The band with larger angle corresponds to the opposite sign

pair partners. The band with smaller angle corresponds to the same sign pair partners and beam particles. The deflection angle for opposite sign pair particle is up to 100 mrad for energy as low as several hundred MeV.

Table 1. Beam Parameters Used for Simulation.

P_b (MW)	$N(10^8)$	f_c (kHz)	ε_y (nm)	β_y (μm)	σ_y (nm)	σ_z (μm)
20	1.6	156	25	62	0.56	1

Table 2. Results Given by the Formulas.

Υ	D_y	n_γ	δ_E	n_b	n_v	$\mathcal{L}_g(10^{35}\text{cm}^{-2}\text{s}^{-1})$
631	0.29	0.72	0.2	0.094	0.026	1

Table 3. Results Given by CAIN Simulations.

n_γ	δ_E	σ_e/E_b	n_b	$\mathcal{L}/\mathcal{L}_g(W_{\text{cm}} \in 1\%)$	$\mathcal{L}/\mathcal{L}_g(W_{\text{cm}} \in 10\%)$
0.97	0.26	0.36	0.12	0.65	0.80

Because of the angle-energy correlation, the number of detector hits by the charged particles may be further reduced with a solenoid magnetic field along the beam pass. In this situation, rather than particle energy, a more relevant variable is transverse momentum, P_t , which determines the radius of the helical orbit in given solenoid field. The angle- P_t distributions of coherent pairs and beam particles are shown in Figure 3 (bottom). Here again the band with larger angle corresponds to the opposite sign pair partners. On this plot, only those particles in the top right corner with large enough angle and P_t will fall outside of a given forward cone and have a chance of hitting the detector directly. The detector planned for NLC has a half cone angle of 100 mrad²¹, seemingly large enough to swallow all coherent pairs and photons for our case.

Coherent pairs can also be produced from virtual photons (as opposed to real photons from beamstrahlung) through a process known as trident cascade. The current version of CAIN does not include this process, but its production rate can be estimated with a simple formula^{1,20}

$$n_v = \left(\frac{\alpha \sigma_z \Upsilon}{\lambda_c \gamma} \right) \Omega(\Upsilon) \quad (21)$$

$$\Omega(\Upsilon) = 0.23 \alpha \log \Upsilon \quad (\Upsilon \gg 1) \quad (22)$$

where the number of pairs per primary particle, n_v , is somewhat lower than the real photon pair production for our case seen from Table 2 and Table 3. Recently Thompson and Chen²² have checked this process in more detail for our parameter set and found it does not seem to cause extra problems.

In addition to coherent pairs produced in collective beam field, incoherent pairs can also be created through individual particle-particle scattering processes. The following processes are included in the simulation: Breit-Wheeler: ($\gamma + \gamma \rightarrow e^+ + e^-$); Bethe-Heitler: ($\gamma + e^\pm \rightarrow e^\pm + e^+ + e^-$); and Landau-Lifshitz: ($e^+ + e^- \rightarrow e^+ + e^- + e^+ + e^-$). Figure 4 shows the scatter plot of incoherent pairs (without beam particles) in angle-energy space (top) and in angle- P_t space (bottom). The simulation used a 10 MeV cut on pair member energy. The two bands seen in the top plot corresponds to the opposite sign partners in the larger angle region and the same sign partners in the smaller angle region. Similarly, in the bottom plot the band with larger angle on the right corresponds to opposite sign partners. Comparing with the coherent pair distribution, incoherent pairs spread much more to the lower energy region and thus are deflected to larger angles. However the total number of incoherent pairs, about 5 thousands for our case, is more than 3 orders of magnitude below that of the coherent pairs. In fact each macro-particle in this Figure corresponds to a real pair particle. With angle and P_t cuts similar to NLC case²¹ the situation here does not seem to be much worse than the 0.5 TeV machine.

5 Major Issues and Uncertainties

A major issue involved in establishing QSB as an IP approach is the assessment of various sources of backgrounds. We have shown in the preceding section that collision products from QED processes could all be confined within a cone of reasonable opening angle. However, the detector may still be affected by the secondary particles generated by the spent beam hitting other components such as quadrupole magnets within the forward cone. In addition, the spent beam may induce damage or even radioactivation on these components. A detailed analysis of these issues requires more specific detector design and realistic detector simulation, which are beyond the scope of this paper. It is hoped the situation could somehow be managed with appropriate masking scheme and IR design.

Collisions of beamstrahlung photons can also produce hadronic minijets through QCD interaction^{23,24,25}, giving rise to yet another source of backgrounds. Current theories on minijets are model dependent with free parame-

ters that need to be adjusted with input from experimental data, so far available only up to 100 GeV. As a result, minijet cross sections based on these theories are nowhere near converging when extrapolating to multi-TeV energy.

Using Drees and Godbole²³ model for minijet cross section, Ohgaki²⁶ recently has carried out a complete case study of hadronic backgrounds for our parameter set, from IP simulation to hadronic event generation to detector simulation. It is found that both number of hadronic events and energy deposition on detector are quite large. However, it is also found²⁷ that some alternative models could give a cross section two orders of magnitude smaller, thus reducing the hadronic backgrounds into an acceptable level. It is therefore the area of uncertainty, where a more definitive prediction on minijet cross section is in urgent need. Suggestions have been made on how to reduce sources of uncertainty and extend the valid regime of the theory to much higher energy²⁵. It is hoped that the improvement could be done shortly.

Last but not least, backgrounds due to standard model processes, such as W pair production in two-photon collisions, also have to be dealt with for exploration of physics beyond the standard model^{16,28}.

6 Conclusions

Constrained by the sheer size and cost of a modern collider, scaling of current technology and approach to higher energy is becoming prohibitive. Thus more than ever before, the future of high energy colliders will depend critically on innovative concepts and techniques, and more important on the successful integration of these concepts and techniques into a collider system, from acceleration to collision, to detection, and all the way to the origination of a discovery experiment. Should the approach of quantum suppression of beamstrahlung be proven acceptable for high energy physics community and viable technically, it will make a strong scientific case with potentially significant strategic value for the future developments of high energy physics and accelerator technology.

Acknowledgments

The author wishes to extend his many thanks to K. Yokoya for help on understanding and using the simulation code CAIN; to J. Siegrist for making available the computer facility with which the simulations for this paper were performed; to S. Chattopadhyay, J. Siegrist and B. Barletta for program support; to K. Yokoya, T. Tajima, S. Chattopadhyay, K.-J. Kim, T. Ohgaki, H. Murayama, J. Siegrist and P. Chen for helpful comments and discussions. This work was supported by the U.S. Department of Energy under contract No. DE-AC03-76SF00098.

References

1. For a comprehensive review, see K. Yokoya and P. Chen, *Frontiers of Particle Beams: Intensity Limitations*, Lecture notes in Physics, 400, eds. M. Dienes et al., (Springer-Verlag, 1992).
2. T. Himel and J. Siegrist, *AIP Conf. Proc.*, **130**, 602(1985).
3. K. Yokoya, *Nucl. Instrum. Methods A***251**, 1(1986).
4. R. Noble, *Nucl. Instrum. Methods A***256**, 427(1987).
5. V. Baier, V. Katkov and V. Strakhovenko, INP-preprint 88-168, Novosibirsk, (1988).
6. P. Chen and K. Yokoya, *Phys. Rev. Lett.*, **61**, 1101(1988).
7. R. Blankenbecler and S. Drell, *Phys. Rev. D*, **37**, 3308(1988).
8. M. Jacob and T. Wu, *Nucl. Phys.*, **B318**, 53(1989).
9. International Linear Collider Technical Review Committee Report, SLAC-R-95-471, (1995).
10. Proceedings of 1996 DPF/DPB Summer Study on New Directions for High Energy Physics, Snowmass, Colorado, (1996).
11. Proceedings of the 1996 Workshop on Advanced Accelerator Concepts, AIP conference Proceedings 398, (1996).
12. N. Solyak, INP-preprint 88-44, Novosibirsk, (1988).
13. J. Rosenzweig, B. Autin and P. Chen, *AIP Conf. Proc.*, **193**, (1989).
14. D. Whittum, A. Sessler, J. Stewart and S. Yu, LBL-25759, (1989).
15. V. Telnov, *Nucl. Instrum. Methods A***294**, 72 (1990).
16. H. Murayama and M. Peskin, *Ann. Rev. Nucl. Part. Sci.* **46**, 533(1996).
17. A. Sokolov, N. Klepikov and I. Ternov, *Soviet Phys. Doklady*, **89**, 665(1953).
18. M. Xie, T. Tajima, K. Yokoya and S. Chattopadhyay, *AIP Conf. Proc.*, **398**, 233(1997).
19. P. Chen, T. Ohgaki, A. Spitkovsky, T. Takahashi and K. Yokoya, *Nucl. Instrum. Methods A***397**, 458 (1997).
20. P. Chen and V. Telnov, *Phys. Rev. Lett.*, **63**, 1796(1989).
21. Zeroth-order design report for the NLC, SLAC Report-474, (1996).
22. K. Thompson and P. Chen, These Proceedings.
23. M. Drees and R. Godbole *Phys. Rev. Lett.* **67**, 1189 (1991).
24. P. Chen, T. Barklow, and M. Peskin. *Phys. Rev. D* **49**, 3209 (1994).
25. R. Godbole, These Proceedings.
26. T. Ohgaki, These Proceedings.
27. T. Ohgaki, private communications.
28. H. Murayama, Talk presented at the mini-workshop on IP physics for linear colliders, LBNL, January, 1998.

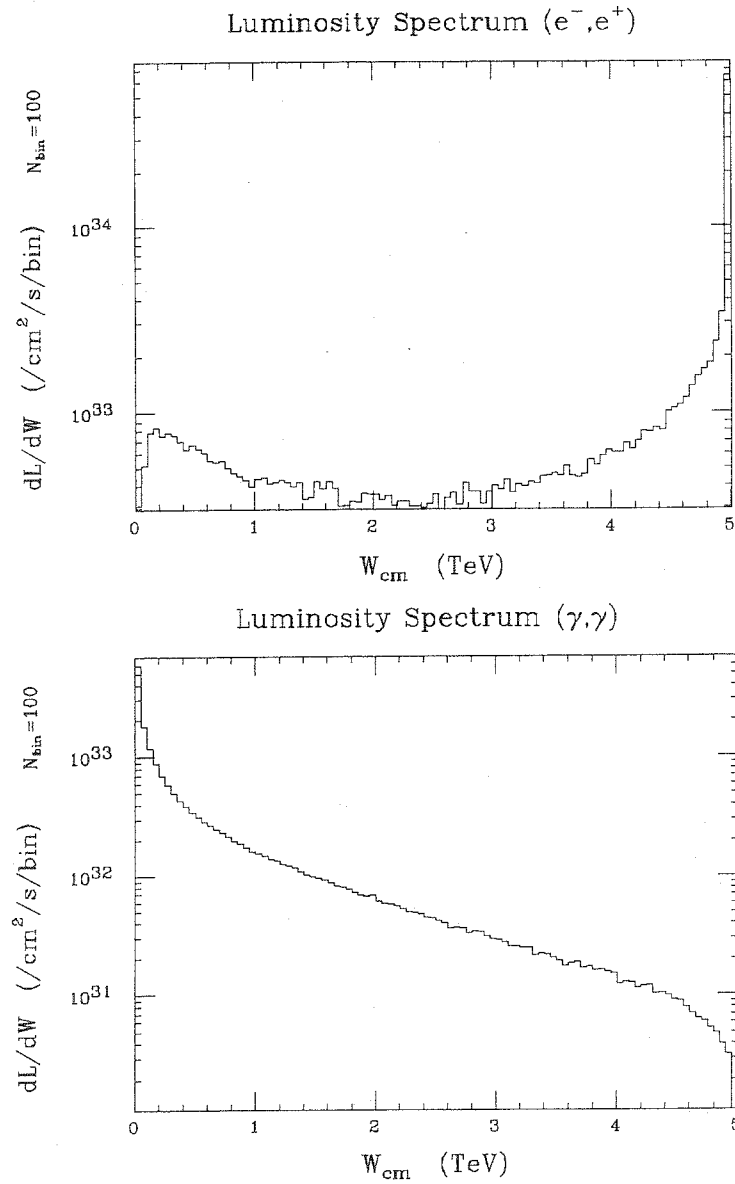


Figure 1: Luminosity spectrum for e^+e^- (top), and $\gamma\gamma$ (bottom). Both with 100 bins.

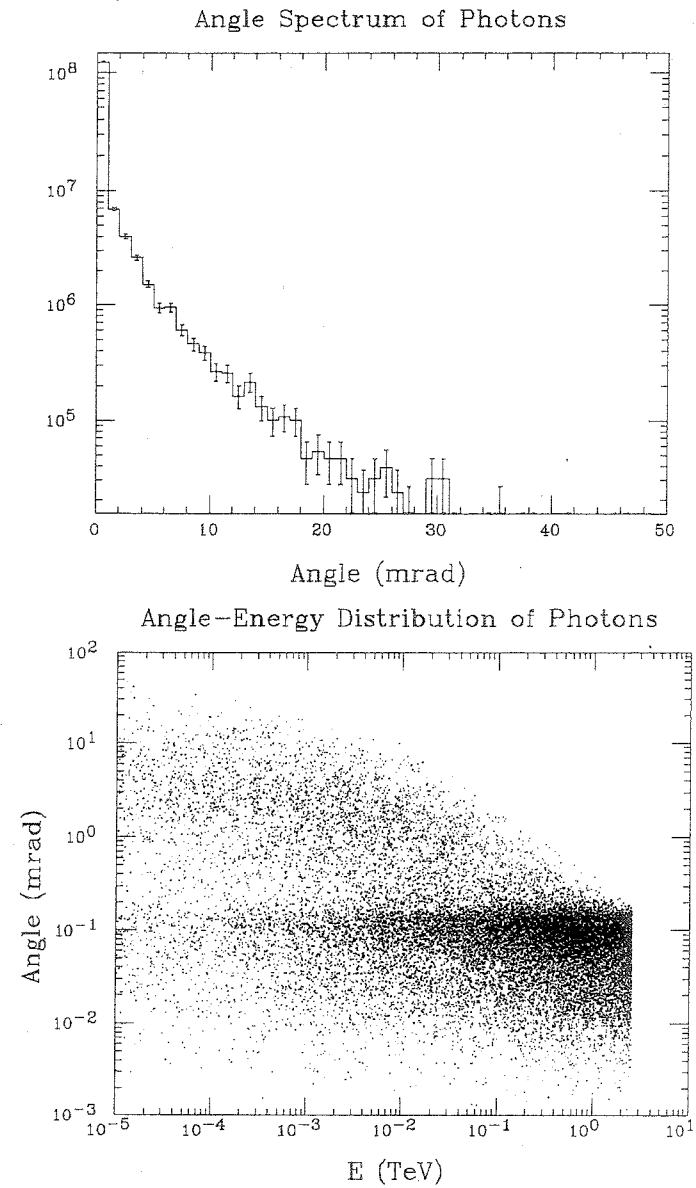


Figure 2: Angle spectrum of photons with bin size of 1 mrad (top). Scatter plot of photons in angle-energy space (bottom).

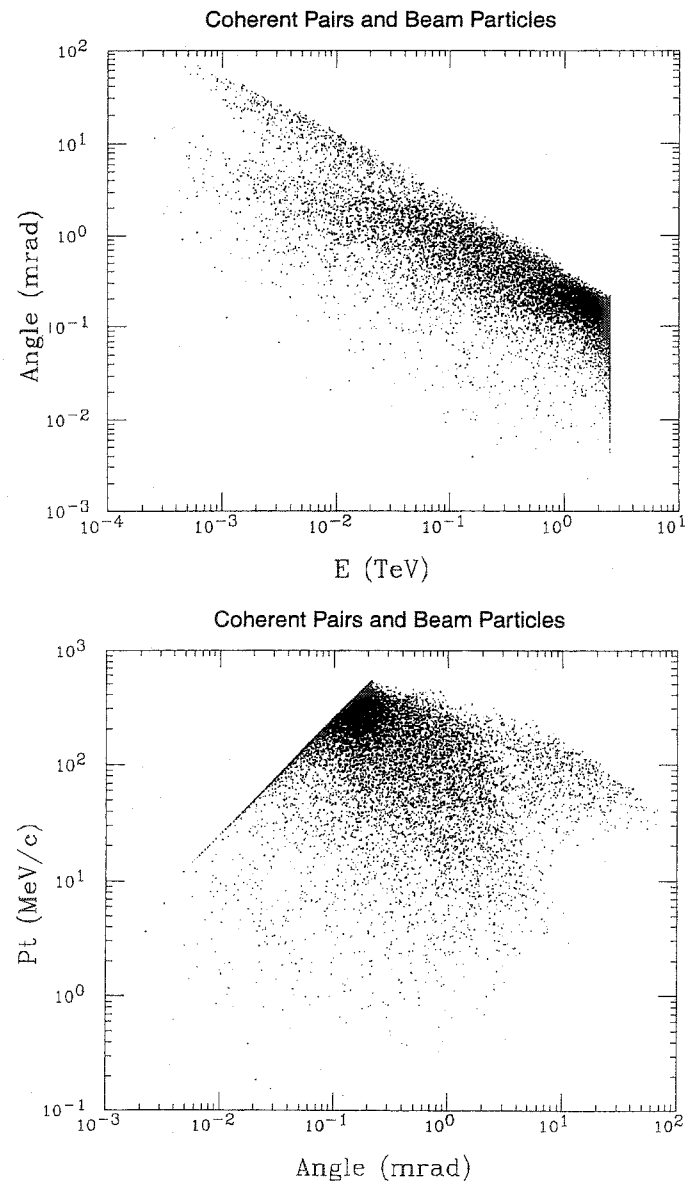


Figure 3: Scatter plot of coherent pairs and beam particles in angle-energy space (top) and in angle- P_t space (bottom).

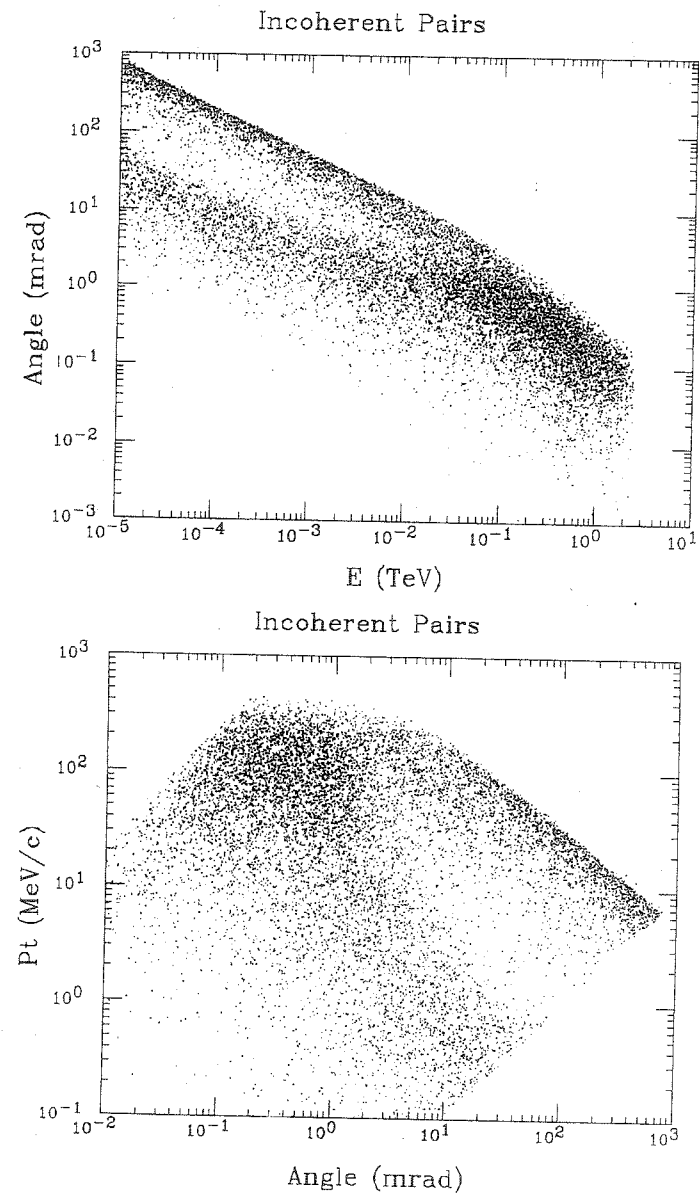


Figure 4: Scatter plot of incoherent pairs in angle-energy space (top) and in angle- P_t space (bottom).